Available online at www.sciencedirect.com
SCIENCE DIRECT®
Coordination Chemistry Reviews 242 (2003) 47–58
COORDINATION CHEMISTRY REVIEWS
www.elsevier.com/locate/ccr

Hierarchical structure in assemblies of enantiopure ruthenium trisdiimine complexes: a biomimetic approach utilizing primary, secondary, tertiary and quaternary structural elements

Frederick M. MacDonnell *, Mahn-Jong Kim, Kelly L. Wouters, Rama Konduri

Department of Chemistry and Biochemistry, The University of Texas at Arlington, Arlington, TX 76019, USA

Received 6 November 2002; accepted 26 February 2003

Contents

Abstract

Rigid, diastereomerically-pure and enantiomerically-pure polynuclear and dendritic assemblies of ruthenium(II)trisphenanthroline complexes show a structural complexity that mimics some of the structural hierarchy found in biological systems. Hexanuclear (**Ru_6**) and decanuclear (**Ru_{10}**) assemblies show a discernable and tunable primary, secondary and tertiary structure. Solution electric birefringence studies of colloids formed from various stereoisomers **Ru_6** or **Ru_{10}** show dramatic and distinctive differences between isomers with differing tertiary structure; indicating, in effect, that different quaternary structures (colloidal structures) are formed as a function of tertiary structure. New synthetic approaches to tune the Ru to Ru distance, to change the geometry of the core (new structural motifs) and to develop a convergent approach to even higher nuclearity dendrimers are presented.

Keywords: Ruthenium; Polypyridyl; Chiral; Dendrimer; Biomimetic; Hierarchical structure

1. Introduction

Biological systems have long since perfected nanochemistry and nanoengineering [1]. The cellular structure and machinery is based, to a significant extent, on the formation of nanometer to micron-sized assemblies of proteins. These magnificent architectures are a result of a hierarchical structural strategy involving primary, secondary, tertiary and even quaternary structural elements to bridge the gap from the molecular to the microscopic [2,3]. The beauty of this strategy is that a relatively simple set of building blocks can lead to a wide-range of diverse structures and functionality. Supramolecular chemistry describes man's efforts to mimic the last two steps of the hierarchical strategy, namely the use of non-covalent linkages to organize discrete molecules into ever-larger architectures [4,5]. Supramolecular organization of polymeric [6] and dendritic materials [7] has been shown to have dramatic and important effects on the electronic and photonic

* Corresponding author. Tel.: +1-817-272-2972; fax: +1-817-272-3808.
E-mail address: macdonn@uta.edu (F.M. MacDonnell).

0010-8545/03/$ - see front matter © 2003 Elsevier B.V. All rights reserved.
doi:10.1016/S0010-8545(03)00027-4

properties of these materials [8] (e.g. carrier mobility increasing by a factor of 10^4 upon self-assembly of conducting polymers as opposed to disordered structures [6]).

One important aspect of the biomimetic strategy, however, has not been fully realized. Nature uses nanometer-sized proteins as building blocks for quaternary structures and these building blocks have various surface recognition groups juxtaposed over nanometer distances, which helps direct their self-assembly into well-defined quaternary structures. Most supramolecular building blocks are either small and rigid (molecular) [5,9,10] or large and floppy (dendrimers, polymers) [11–19], and therefore, fail to fully emulate the structural integrity of a well-folded protein with a discernable tertiary structure on the nanometer scale.

We have developed a method of constructing conformationally-rigid, nanometer-sized dendritic complexes, which exhibit a discernable and tunable tertiary structure on the nanometer scale [20,21]. Chemically robust ruthenium(II) trisphenanthroline complexes, shown in Fig. 1, form the basic building block—in this case analogous to amino acids. We have only two types of building blocks, the enantiomers of $[Ru(phen)_3]^{2+}$ (and closely related derivatives) which are labeled Δ and Λ to denote the chirality at the metal center. These enantiomers are separable and are stable. When linked together in a rigid and stereospecific manner (as indicated in Fig. 1) the absolute chirality (the primary structural element) directs the orientation of the larger (>3 nm) triangular structures of four rutheniums, **Ru_4** (secondary structural elements) with respect to another interlocked triangle(s). Two such **Ru_4** triangles are interlocked (each sharing the two central Ru centers) to give either a flat hexamer (Fig. 1, left bottom) or twisted bow-tie type hexamer (Fig. 1, right bottom) in which the global topology (tertiary structure) is precisely defined over dimensions from 4.2 nm [20,21]. Solution studies of these hexamers (**Ru_6**) and related decamers (**Ru_{10}**) have shown that the colloidal structure of such dendrimers depends dramatically on the tertiary

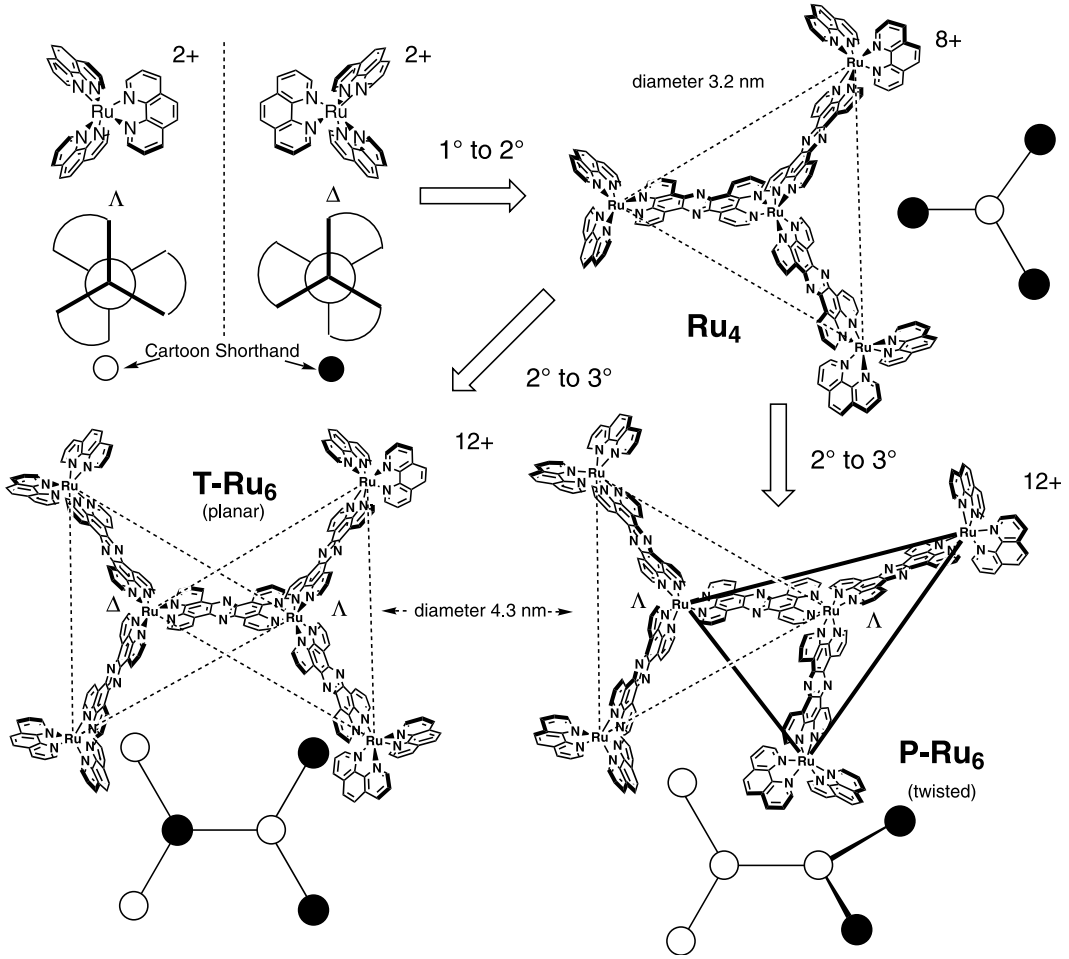

Fig. 1. Structure and mirror image relationship of chiral Ru(II) trisphenanthroline building blocks, their assembly into rigid tetramers (**Ru_4**), and a conceptual schematic as to how such tetramers can be linked to form hexamers (**Ru_6**) with differing tertiary structures. Ball and stick figures are shorthand for the polynuclear assemblies with white and black balls indicating Λ and Δ stereocenters, respectively.

structure of the dendrimer, thus showing 'quaternary' structure to extend the analogy with biology [22].

These ruthenium complexes have the added benefit of being extraordinarily chemically robust (easily manipulated/stable), electronically and photophysically interesting (accessible redox and photoexcited states), and chiral (potential for chirooptical and chiral recognition applications). While our work is still developing, we believe this synthetic approach offers a unique platform for organizing and assembling nanometer-sized molecules over much larger distances. In this review, we give an overview of our synthetic approach, describe some of the physical studies used to examine this system and indicate the new directions this research is leading to.

2. Primary and secondary structure

2.1. Preset chiral synthons for supramolecular syntheses

The ruthenium(II)trisphenanthroline complex can be viewed as a chiral synthon which has both a threefold symmetry axis (a three bladed propeller) and three twofold symmetry axes perpendicular to the C_3 axis. In order to utilize the full symmetry of the building block and to restrict rotational and conformational motion, we pursued a coupling strategy as shown in Fig. 2. The peripheral dione and diamine functions undergo a high yield ($>90\%$) condensation reaction to form a rigid tpphz bridge between monomers [23] to give a

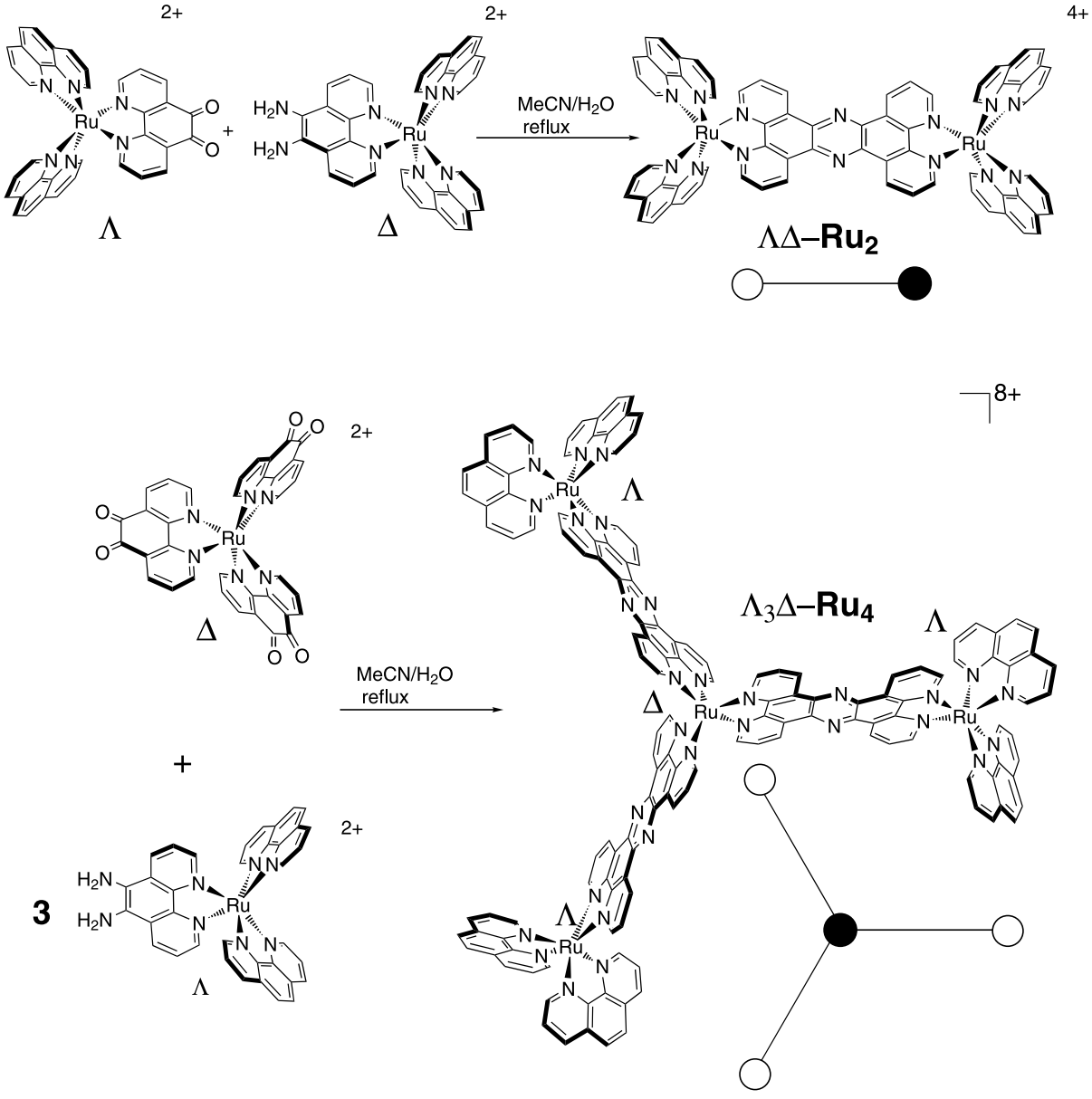

Fig. 2. Stereospecific syntheses of the meso ΛΔ-**Ru$_2$** and heterochiral $\Lambda_3\Delta$-**Ru$_4$**.

dimer (modified along one C_2 axis) or tetramer (modified along all three axes). The resulting structures are large with diameters estimated at 1.6 nm for **Ru_2** and 3.2 nm for **Ru_4**. The triangular symmetry of the tetramer **Ru_4** is a reflection of the underlying threefold symmetry at the core. In fact, this structure is essentially planar, with all four Ru(II) ions lying in the same plane. As described earlier, these triangles are our secondary structural elements (four adjacent points always form a planar triangle) from which we form the larger tertiary structures observed in the hexamers and decamers. We will use the ball and stick drawings of the type shown in Figs. 1 and 2 to represent these and larger structures. White and black balls indicate a Λ-$[Ru(phen)_3]^{2+}$ or Δ-$[Ru(phen)_3]^{2+}$ stereocenter, respectively, while the line joining the two balls indicates the formation of a tpphz bridge between them and the Ru–Ru distance is known from crystallography to be 12.7 Å [24]. Different stereoisomers of these complexes are readily prepared in diastereomerically-pure (dp) and enantiomerically-pure (ep) form because the monomeric precursors are enantiomerically-pure. For example, ΛΛ-**Ru_2** can be generated by combining Λ-$[Ru(phen)_2$(phen-5,6-dione)$]^{2+}$ and Λ-$[Ru(phen)_2$(phen-5,6-diamine)$]^{2+}$.

NMR studies using chiral lanthanide shift reagents have shown that despite often harsh reaction conditions, the $[Ru(phen)_3]^{2+}$ unit is not racemized under the conditions used to assemble these dendrimers. Recently, we, in collaboration with a group at Furman University, have used extended the use of capillary electrophoresis (CE) in the presence of chiral anions to examine the stereochemical integrity monomers [25] to the dimers. Samples of the homochiral (ΛΛ and ΔΔ) isomers of Ru_2 were compared with a "racemic" mixture of ΛΛ-Ru_2 and ΔΔ-Ru_2. The CE traces, shown in Fig. 3, indicate little or no presence of the opposite isomer in either case. This is further evidence of both the effectiveness of the resolution procedure as well as the absence of any racemization occurring during the coupling reaction.

While synthesis of the homochiral ruthenium dimers, ΔΔ-**Ru_2** or ΛΛ-**Ru_2**, were straightforward, attempts to generate pure meso dimer (ΛΔ-**Ru_2**) proved more troublesome. The meso dimer formed from the coupling of Δ-$[Ru(phen)$(phen-5,6-dione)$]^{2+}$ and Λ-$[Ru(phen)$-(phen-5,6-diamine)$]^{2+}$ was always observed to show the presence of some homochiral dimer (ΛΛ-**Ru_2**) by circular dichroism (CD) analysis. It was also observed that the homochiral impurity was always of the same enantiomeric identity as the diamine precursor. Ultimately, we discovered a redox side-reaction (see Fig. 4) in which some of the Λ-$[Ru(phen)_2$(phen-5,6-diamine)$]^{2+}$ is oxidized by the quinone to generate $[Ru(phen)_2$(phen-5,6-diimine)$]^{2+}$. This species can react with the remaining Λ-$[Ru(phen)_2$(phen-5,6-diamine)$]^{2+}$ to form the homochiral ruthenium, which constitutes as much as 23% of the final product. Fortunately, a simple

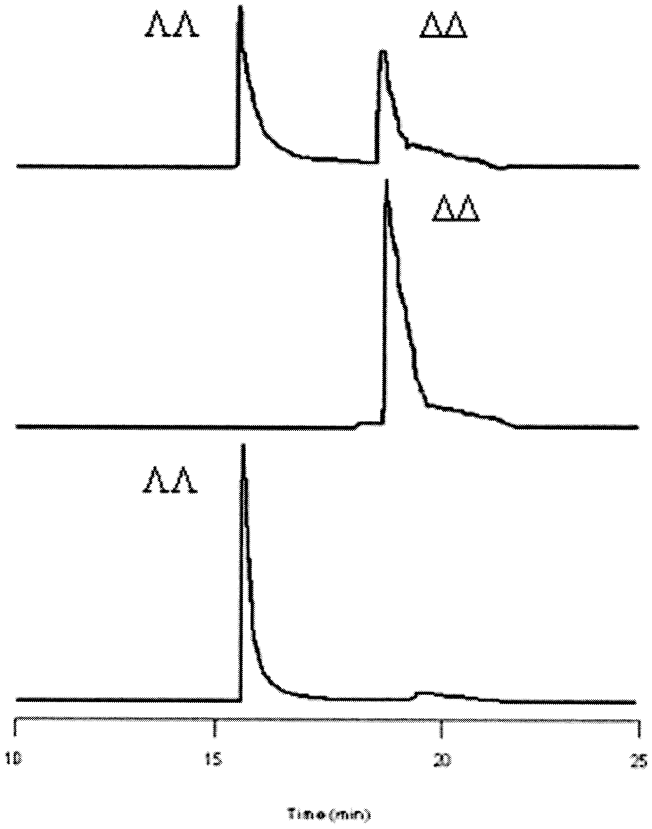

Fig. 3. CE traces of homochiral (ΛΛ and ΔΔ) isomers of **Ru_2** and a prepared 50/50 (racemic) mixture of ΛΛ-**Ru_2** and ΔΔ-**Ru_2** (top). Potassium antimonyl (+)tartrate has been added to the running buffer as the chiral discriminator.

modification of the reaction solvent (addition of acetic acid) results in formation of the meso dimer with less than 5% of the homochiral contaminant [26].

This synthetic system is also flexible and not restricted to only the tpphz bridging ligand. Dimers such as $[(phen)_2Ru(tatpp)Ru(phen)_2]^{4+}$ and $[(phen)_2Ru$-$(tatpq)Ru(phen)_2]^{4+}$ (shown in Fig. 5, top) which have a Ru–Ru distance of 17 Å have been made in a stereospecific manner [27] and incorporate some interesting multi-electron photochemistry [28,29]. A trimer bridged by the PHAT ligand is formed upon condensation of three equivalents of $[Ru(phen)_2$(phen-5,6-diamine$]^{2+}$ with hexaketocyclohexane octahydrate as shown in Fig. 5 (bottom). Lehn and coworkers have previously reported the stereospecific syntheses of this trimer [30], however, the present route offers higher yields of this important potential core molecule for higher nuclearity dendrimers [27].

With these synthetic tools, it is possible to generate a large number of dendritic structures with targeted stereochemical compositions which ultimately will direct the global or tertiary structure in the larger assemblies.

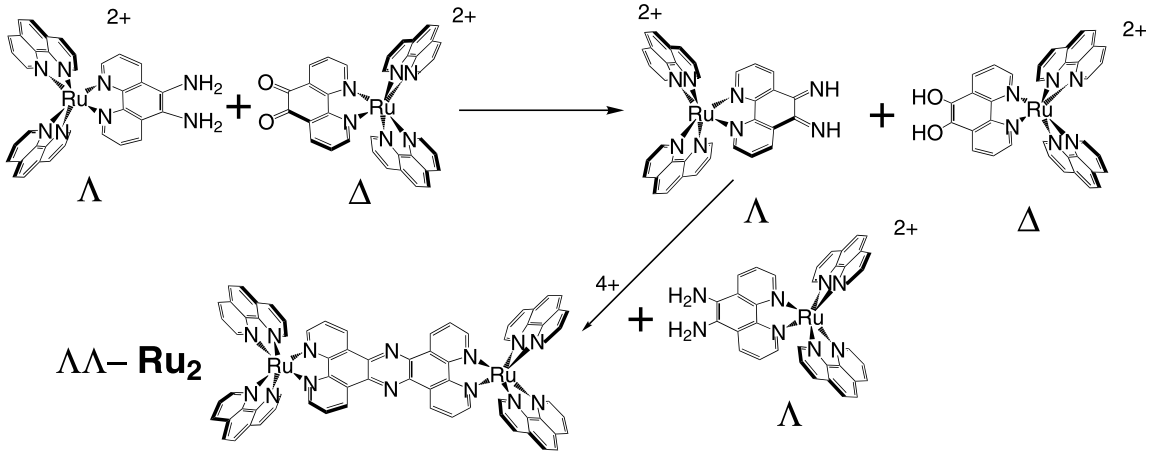

Fig. 4. Redox side reaction of Λ-[Ru(phen)$_2$(phen-5,6-diamine)]$^{2+}$ and Δ-[Ru(phen)$_2$(phen-5,6-dione)]$^{2+}$ to give ΛΛ-**Ru$_2$**.

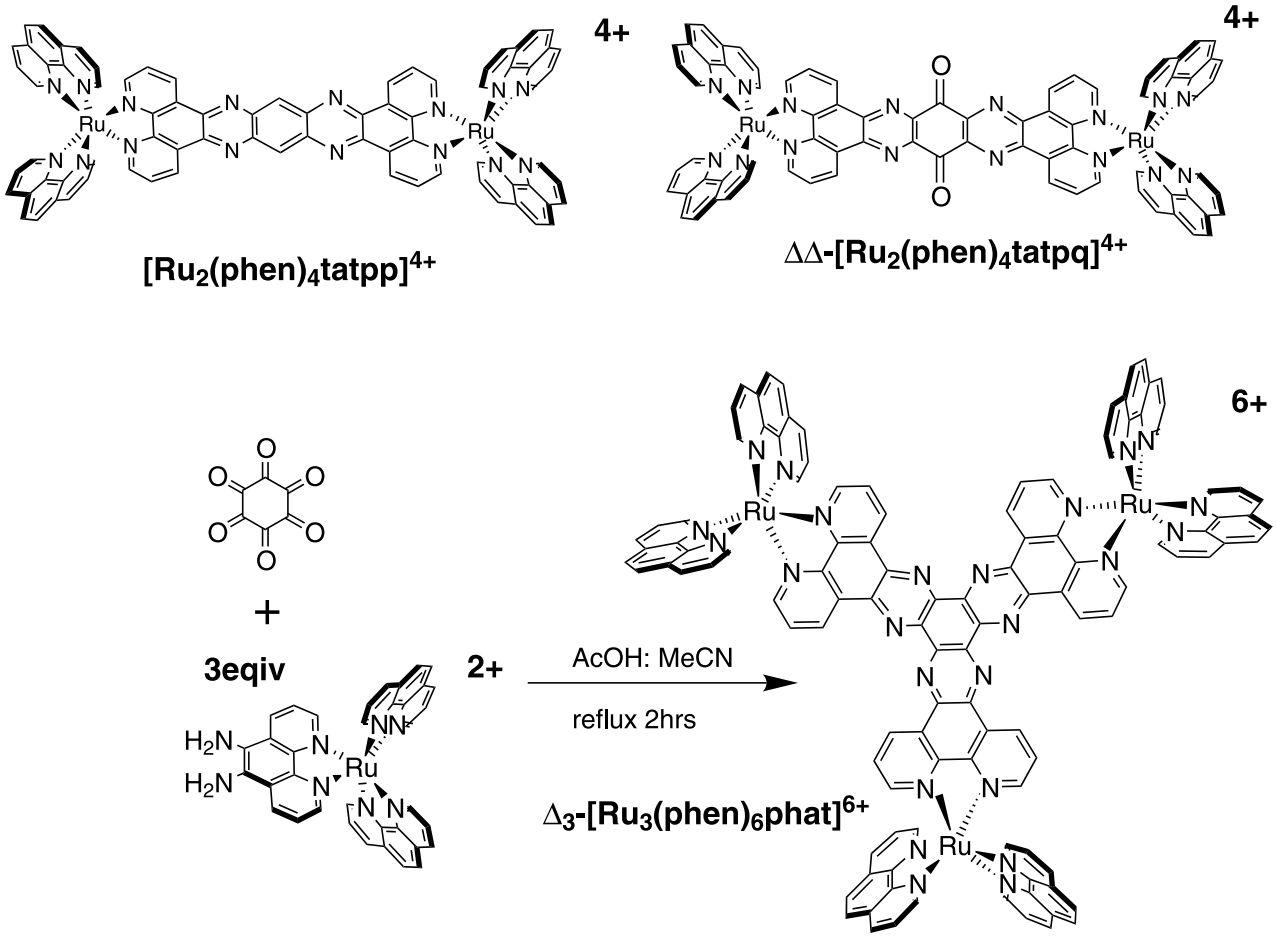

Fig. 5. Homochiral dimmers, ΔΔ-[Ru$_2$(phen)$_4$(tatpp)]$^{4+}$ and ΔΔ-[Ru$_2$(phen)$_4$(tatpq)]$^{4+}$ (top), and stereospecific synthesis of homochiral trimer, Δ$_3$-[Ru$_3$(phen)$_6$(phat)]$^{6+}$ (bottom).

2.2. Stereospecific syntheses dendritic hexamers and decamers

The formation of two hexameric structures by interlinking two triangular tetramers (**Ru$_4$**) was shown in Fig. 1 in a conceptual manner only. In order to actually build these larger structures we must use dimers and tetramers as 'core' structures in which the outer phenanthrolines are functionalized with peripheral dione or diamine groups. Fortunately, the oxidation of the peripheral phenanthroline ligands at the 5 and 6 positions is both facile and selective, considering the harsh reaction

conditions (sulfuric acid, nitric acid and NaBr at 100 °C for 20 min) [31–33]. The crude products, **Ru_2one** and **Ru_4one** (where the **-one** suffix indicates conversion of peripheral phenanthrolines to phenanthroline-5,6-dione), are sufficiently clean to be used directly for further dendritic growth. The reaction also leaves the stereochemistry undisturbed as determined using NMR with chiral lanthanide shift reagents [33].

Figs. 1 and 6 show the molecular structures of hexamer and decamer (**Ru_6** and **Ru_{10}**), respectively, as obtained from the reaction of the oxidized dimer (**Ru_2one**) and tetramer (**Ru_4one**, shown in Fig. 6) with a slight stoichiometric excess of $[Ru(phen)_2(phen\text{-}5,6\text{-}diamine)]^{2+}$. Condensation reaction of one equivalent of enantiopure dinuclear complex, ΛΛ-**Ru_2one**, ΔΔ-**Ru_2one** or ΔΛ-**Ru_2one** and 5 equivalent of enantiopure Δ (or Λ)-$[(phen)_2Ru(phendiamine)]^{2+}$ gave six different ep and dp pure isomers $\Lambda_4\Lambda_2$-**Ru_6**, $\Delta_4\Delta_2$-**Ru_6**, $\Lambda_4\Delta_2$-**Ru_6**, $\Delta_4\Lambda_2$-**Ru_6**, $\Delta_4(\Lambda\Delta)$-**Ru_6** and $\Lambda_4(\Lambda\Delta)$-**Ru_6** [34]. The notation used above (e.g. $\Lambda_4\Delta_2$-**Ru_6**) gives the stereochem-

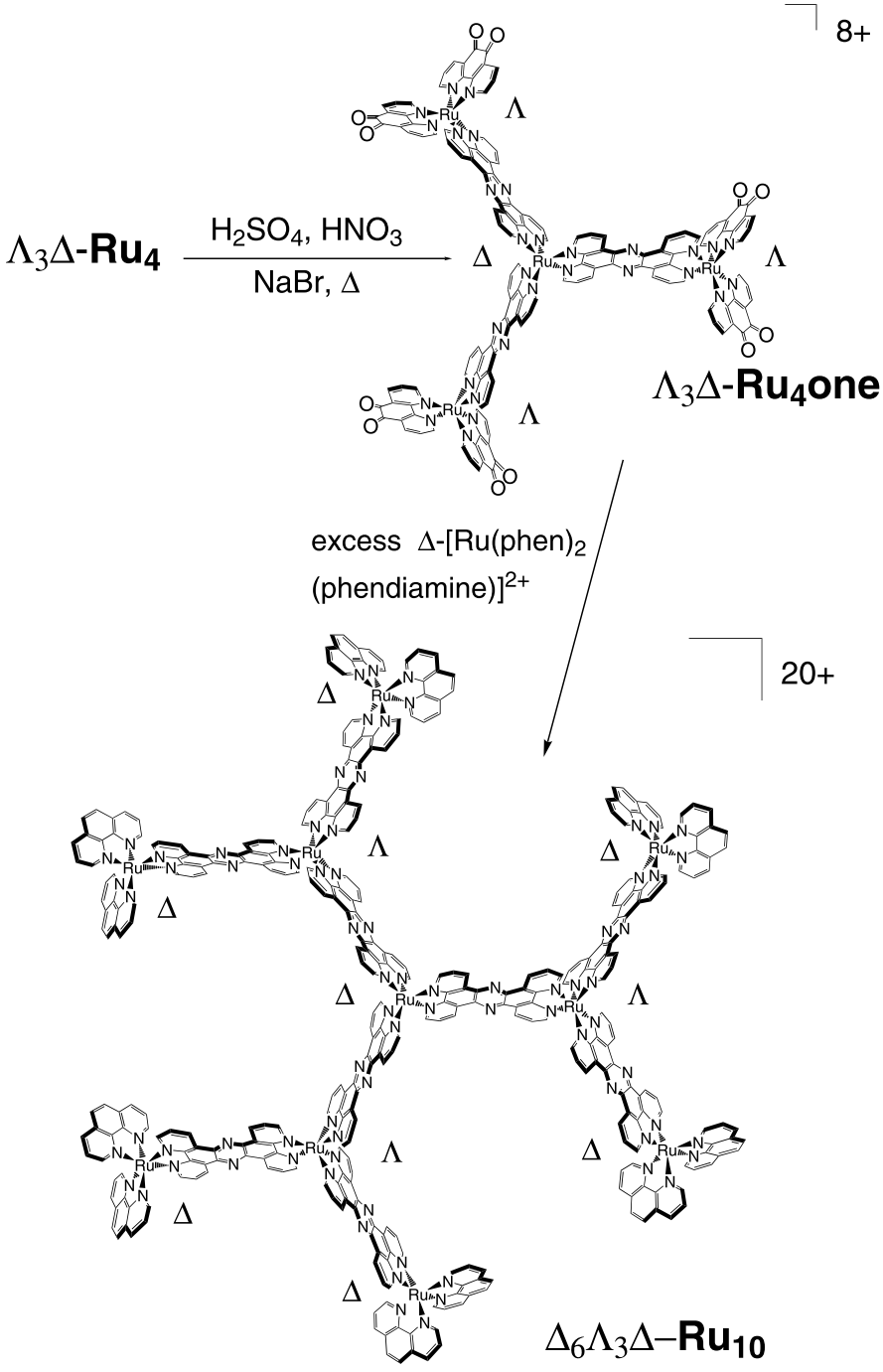

Fig. 6. Oxidation of the tetramer (**Ru_4**) to **Ru_4one** and stereospecific synthesis of the decamer, $\Delta_6\Lambda_3\Delta$-**Ru_{10}**.

istry of the peripheral rutheniums first, then and then the core sites. Of the possible stereoisomers for the decamers, only four, $\Lambda_6\Lambda_3\Lambda$-**Ru$_{10}$**, $\Lambda_6\Delta_3\Lambda$-**Ru$_{10}$**, $\Delta_6\Delta_3\Delta$-**Ru$_{10}$** and $\Delta_6\Lambda_3\Delta$-**Ru$_{10}$**, have been prepared thus far. All complexes have been characterized via a combination of 1- and 2-D NMR, electrospray and/or MALDI mass spectrometry, and elemental analyses [22,34]. We should note that all of these multinuclear assemblies are highly charged cations with **Ru$_6$** and **Ru$_{10}$** carrying a charge of +12 and +20, respectively. Despite the high charge, all of the complexes show good solubility in acetonitrile and DMSO (for the PF_6^- salts) and in water and methanol (for the Cl^- salts).

3. Tertiary structure

To a first approximation, we could view all dimers (**Ru$_2$**) as essentially being similarly shaped rods and all tetramers (**Ru$_4$**) being similarly shaped triangles. These molecules do not exhibit tertiary structure—in a manner analogous to biology—in that only a primary and secondary structural hierarchy are observed. However, their higher congeners (**Ru$_6$** and **Ru$_{10}$**) clearly do. As indicated in Fig. 1, hexameric structures (**Ru$_6$**) can have more than one locked conformation as can other higher nuclearity structures. This variable tertiary structure is a consequence of the way the phenanthrolines line up either staggered or eclipsed when two such stereocenters are rigidly bridged by a ligand such as tpphz. Consider the Newman projection shown in Fig. 7 for the dimer **Ru$_2$**. When the dimer is viewed down the long Ru–Ru axis, (see arrow) we observe that when the Ru stereocenters are heterochiral (Δ–Λ) the terminal phenanthroline rings are eclipsed (bottom left), however, for the homochiral $\Lambda\Lambda$ dimer, front and back phenanthroline rings are now staggered (bottom right). As indicated by the arrows in Fig. 7, these terminal phenanthrolines are the vectors along which additional stereocenters are added to make, for example, **Ru$_6$**. If four Ru stereocenters are added (along each phen axis), the resulting hexamers (**Ru$_6$**, see Fig. 8) will be either planar or twisted. In fact, since the twist angle is not 90° but instead 72° two enantiomorphic twisted structures result depending on whether the two core ruthenium stereocenters are both Λ or Δ. The macroscopic pitch angle is a direct consequence of the local 36° pitch angle relative to the C_3 axis found for the $[Ru(phen)_3]^{2+}$ synthons [35]. When they are $\Lambda\Lambda$, the resulting hexamer has a right-handed twist denoted by the chiral descriptor **P** and when they are $\Delta\Delta$ the descriptor **M** is used. When a $\Delta\Lambda$ (or meso) core is used a non-twisted, flat structure results and is denoted by a **T** stereochemical descriptor [21]. Thus the three tertiary structures for the hexamers are quickly represented as **P-Ru$_6$**, **M-Ru$_6$**, and **T-Ru$_6$** and are shown as determined by molecular modeling and in cartoon form in Fig. 8. These structures were determined from crystallographic data for the $[Ru(phen)_3][PF_6]_2$ structure [36] and molecular modeling [22].

We also observe discrete tertiary structure in the decamers. A total of four isomeric decamers, $\Lambda_6\Lambda_3\Lambda$-

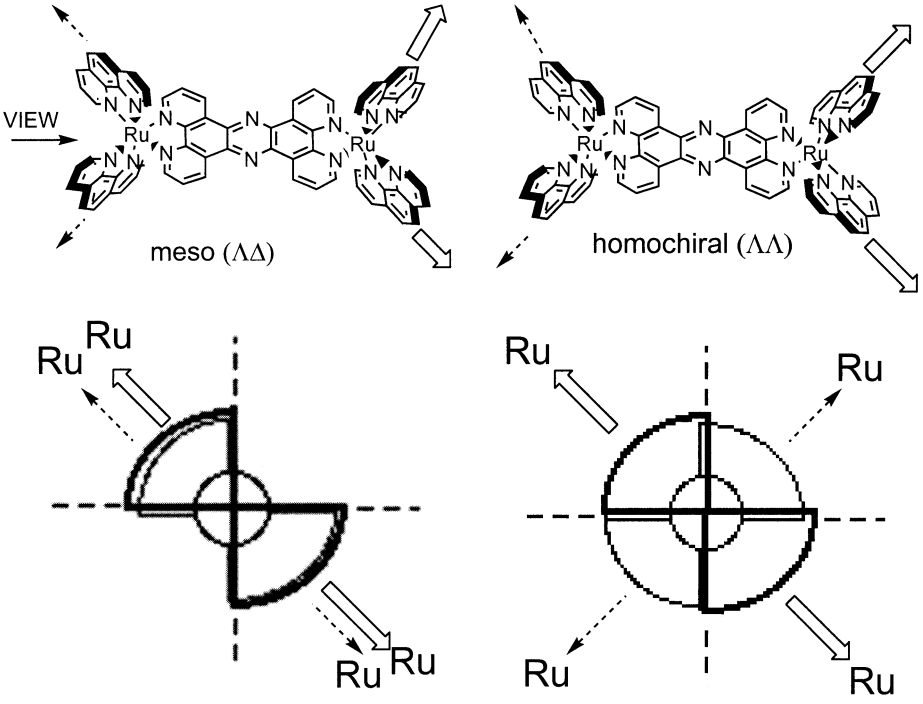

Fig. 7. Newman projections of **Ru$_2$** showing dependence of hexamer (**Ru$_6$**) tertiary structure on local chirality of core.

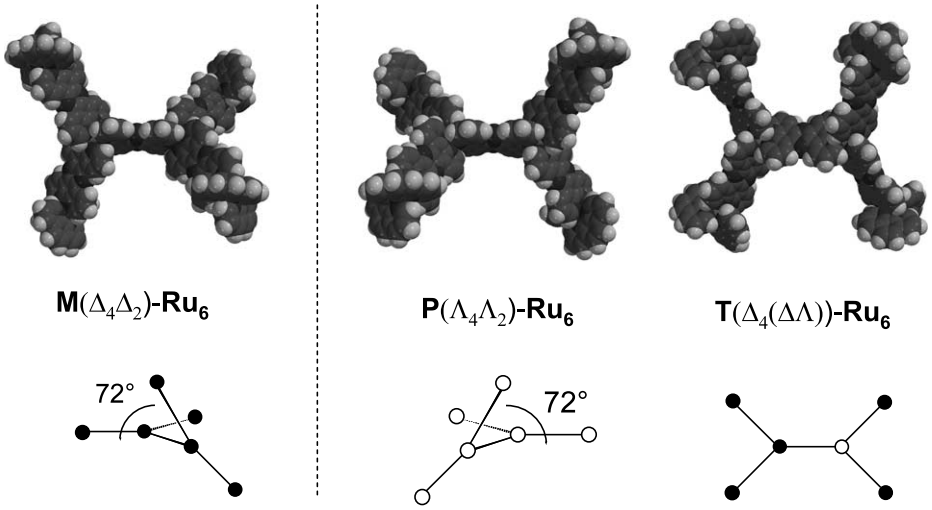

Fig. 8. Space-filling models of **Ru$_6$** showing **P**, **M**, and **T** structures.

Ru$_{10}$, $\Lambda_6\Delta_3\Lambda$-**Ru$_{10}$**, $\Delta_6\Delta_3\Delta$-**Ru$_{10}$** and $\Delta_6\Lambda_3\Delta$-**Ru$_{10}$**, have been prepared [22,34], two of which are shown in Fig. 9. The two isomers differ only in the stereochemistry at three dendritic sites, however as can be seen, this small change in primary structure has a dramatic effect on the overall topology. When viewed from the central Ru core, each arm consists of a plane of four ruthenium centers. For $\Lambda_6\Lambda_3\Lambda$-**Ru$_{10}$**, the pitch angle of this plane relative to the molecular C_3 axis is $\sim 18^\circ$. For $\Lambda_6\Delta_3\Lambda$-**Ru$_{10}$** this pitch angle is 90° resulting in a flat disk-like structure. For the 'flat' or **T** isomer, the all ten Ru atoms lie in the same plane whereas the structure on the right can be viewed as a central four-metal planar unit with the outermost Ru sites above and below this plane resulting in a massive right-handed propeller structure. For the flat **T**-structure, the central and adjacent metal sites have the opposite handedness.

The absorption and CD data at 23 °C for the hexamer and decamer as well as the monomers, dimer and tetramer in deaerated acetonitrile are displayed in Table 1. The absorption spectra of the multinuclear complexes exhibit very intense ligand-centered (LC) bands in the

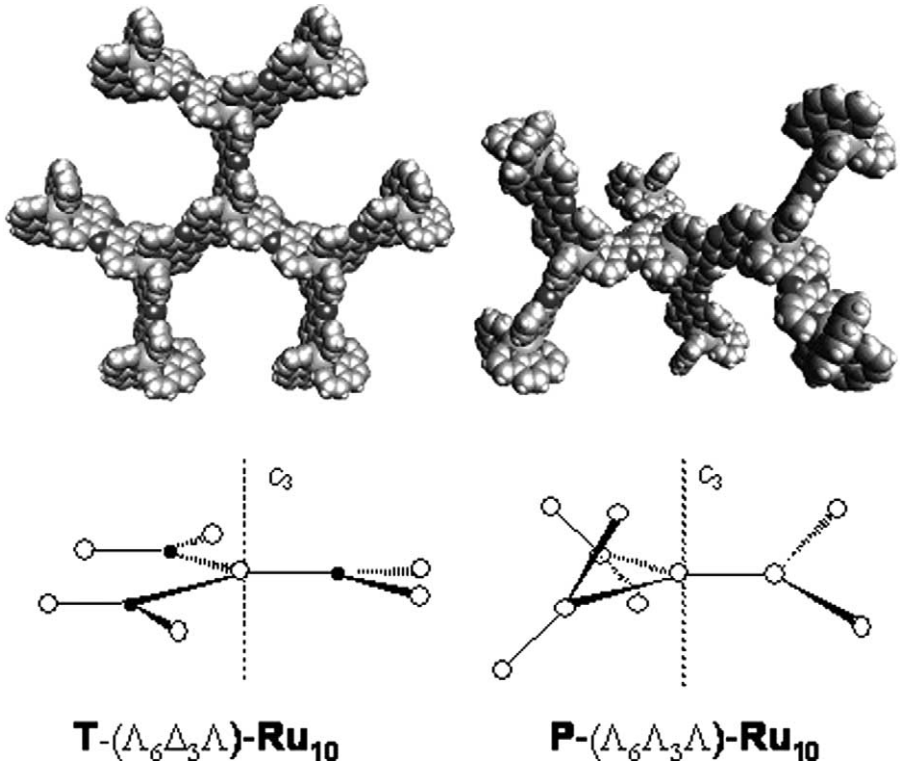

Fig. 9. Space-filling models of **Ru$_{10}$** showing **P** and **T** structures.

Table 1
Selected absorption and CD data of Ru(II) complexes in the MLCT region (MeCN, 298 K)

Complex	Absorption λ_{max} (nm) (ε, M^{-1} cm^{-1})	CD λ_{max} (nm) (Mol. CD)
Dinuclear complexes		
$\Delta\Delta$-**Ru$_2$**	439 (36 500)	470 (−36)
$\Lambda\Lambda$-**Ru$_2$**	438 (35 500)	470 (+36)
$\Delta\Lambda$-**Ru$_2$**	439 (38 100)	490 (+2)
Hexanuclear complexes		
$\Delta_4\Delta_2$-**Ru$_6$**	440 (140 000)	475 (−104)
$\Lambda_4\Lambda_2$-**Ru$_6$**	440 (135 000)	477 (+117)
$\Lambda_4\Delta_2$-**Ru$_6$**	441 (136 000)	464 (+45)
$\Delta_4\Lambda_2$-**Ru$_6$**	441 (138 000)	459 (−44)
$\Delta_4(\Delta\Lambda)$-**Ru$_6$**	440 (138 000)	474 (−78)
$\Lambda_4(\Delta\Lambda)$-**Ru$_6$**	440 (139 000)	470 (+73)
Decanuclear complexes		
$\Delta_6\Delta_3\Delta$-**Ru$_{10}$**	440 (208 000)	483 (−183)
$\Lambda_6\Lambda_3\Lambda$-**Ru$_{10}$**	440 (205 000)	477 (+178)
$\Lambda_6\Delta_3\Lambda$-**Ru$_{10}$**	441 (220 000)	464 (+76)
$\Delta_6\Lambda_3\Delta$-**Ru$_{10}$**	441 (225 000)	467 (−75)

UV region (ε approach to 10^6 M^{-1} cm^{-1}) and intense metal-to-ligand charge-transfer (MLCT) bands in the visible region (ε in the range 100 000–250 000 M^{-1} cm^{-1}). For all isomers of **Ru$_2$**, **Ru$_4$**, **Ru$_6$**, **Ru$_{10}$**,, the extinction coefficient and Cotton effect in the MLCT region are directly proportional to the total number (and stereochemical configuration for CD) of ruthenium chromophores within the structure, showing weak electronic coupling between chromophores. There was no observable difference in the absorption spectrum between isomers of the same nuclearity. Similarly, the magnitude of the CD spectra in the MLCT region for isomers of the same nuclearity could be easily interpreted as proportional to the net number of stereocenters in excess within each complex [21].

4. Quaternary structure

To extend the analogy with biological structural hierarchy, we need to demonstrate that the tertiary structure of the hexamers and decamers affects the type of aggregate structures they can form. We have previously shown that the differing tertiary structures for **T**($\Lambda_6\Delta_3\Lambda$)-**Ru$_{10}$** and **P**($\Lambda_6\Lambda_3\Lambda$)-**Ru$_{10}$** do dramatically affect the colloidal properties as measured by electric birefringence (EB). Campagna and coworkers had previously shown that related metallodendrimers are colloidal in dilute acetonitrile solution [37]. Dynamic light scattering experiments show that both **T**($\Lambda_6\Delta_3\Lambda$)-**Ru$_{10}$** and **P**($\Lambda_6\Lambda_3\Lambda$)-**Ru$_{10}$** exhibit polydisperse aggregation phenomena in acetonitrile (as the hexafluorophosphate salt) and water (as the chloride salt). While no distinction between diastereomers could be observed in the light scattering experiment, both the amplitude and relaxation time for birefringence signals show a distinct difference for the two colloids [22]. For the **T** isomer (74 μM, Cl^- salt in water), the amplitude of the birefringence is small and the corresponding decay signal is fast (on the microsecond timescale). On the other hand, for the **P** isomer (77 μM, Cl^- salt in water) the amplitude of the birefringence is much larger and the decay far slower (on the second timescale).

More recently, we have examined the electric birefringence behavior of **P-** and **T-Ru$_6$**, which may be viewed as the smallest polynuclear species of our to exhibit tertiary structure. As shown in Fig. 10, a marked difference in the EB is observed for the two hexamers with the twisted or **P** isomer again showing a much longer relaxation period (full data not shown) after perturbation by the electric field than the flat **T** isomer.

In order to confirm that these results are a consequence of differing topology and not simply the diastereotopic nature of the complexes, $\Lambda_3\Delta$-**Ru$_4$** and $\Lambda_3\Lambda$-**Ru$_4$** were also examined. These two diastereomers have globally similar molecular topologies and also form polydisperse colloids in aqueous solution. In this control, the birefringence signals were indistinguishable (both 0.22 mM, Cl^- salt in water). It is apparent that under the influence of an electric field, the isotropic solutions of **P-Ru$_{10}$** and **P-Ru$_6$** become optically anisotropic, which is likely due to structural distortion/orientation of the aggregates in the direction of the field E, whereas the rapid evolution of the birefringence for **T-Ru$_{10}$** and **T-Ru$_6$** solutions can be attributed to electronic polarization. We continue to investigate the EB behavior of these hexamers and decamers under a variety of solvent conditions, in the presence of other counterions, and upon forming racemic mixtures of **P** and **M** isomers. We hope that this data will lead to a model of the colloidal structure of these assemblies.

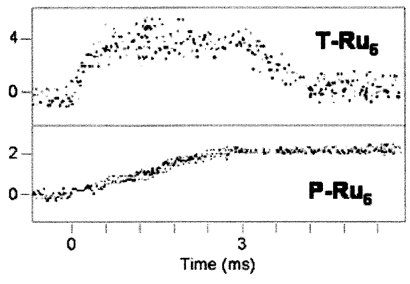

Fig. 10. Plot of electric field-induced birefringence signals (E = 6.4 kV cm^{-1}, pulse length = 3 ms) of **T-**($\Lambda_4(\Delta\Lambda)$)-**Ru$_6$** (top) and **P-**($\Lambda_4\Lambda_2$)-**Ru$_6$** (bottom).

5. Convergent approach to higher nuclearity species

The synthetic approach for the dendrimers can either be divergent or convergent [38]. The hexamers and decamers described so far were obtained using a divergent strategy. However, for high generation dendrimers, a convergent synthesis is desirable for obtaining defect-free structures. Towards this end, we have synthesized a wedge-like trinuclear ruthenium complex, $[((phen)_2Ru(tpphz))Ru(phendiamine)]^{6+}$ (**Ru_3pda**). This trimer was constructed as shown in Fig. 11.

Thus far, our efforts to prepare this trimer in a stereospecific manner have been hampered by the difficulty in controlling the absolute stereochemistry at the apical Ru center. A stereospecific synthesis of trimer depended on the use of the enantiopure complexes of $[Ru(phen)_2py_2]^{2+}$ and $[Ru(phen)_2(phen\text{-}5,6\text{-}diamine)]^{2+}$, both of which are reported in the literature as resolved complexes [23,39,40]. For convenience, we will only describe the preparation of the homochiral Δ trimer. Δ-$[Ru(phen)_2py_2]^{2+}$ could stereospecifically be converted to Δ-$[Ru(phen\text{-}5,6\text{-}dione)_2py_2]^{2+}$ following by oxidation of 5 and 6 positions of the phenanthrolines using reaction conditions described for the preparation of **Ru_2one** and **Ru_4one**. Reaction of this 'core' with two chiral Δ-$[Ru(phen)_2(phendiamine)]^{2+}$ units gives the trimer, $\Delta_2\Delta$-$[((phen)_2Ru(tpphz))Ru(py)_2]^{6+}$ in 82% yield.

Up to this point, the optical purity of the three stereocenters is completely retained as determined by CD and comparison with model reactions, but the next reaction involves a ligand displacement reaction at the apical Ru stereocenter. Displacement of the moderately labile pyridine ligands with 1,10-phenanthroline-5,6-diamine under water–ethanol (90:10) under reflux conditions gave $\Delta_2\Delta$-$((phen)_2Ru(tpphz))Ru(phendiamine)]^{6+}$ in 24% yield, however, the optical purity at the apical center was only 90% optically pure indicating 10% epimerization. Stereospecific substitution of *cis*-pyridine or carbonyl ligands on other enantiopure *cis* $[Ru(diimine)_2L_2]^{2+}$ complexes has been reported by other groups [30,41–48], however, there is some question as to how much racemization occurs. Some groups report 95% retention of optical activity, but Keene and coworkers have shown in a careful study that the degree of racemization is strongly affected by the reaction temperature for these pyridyl and related carbonyl complexes [45]. We are still working to increase the

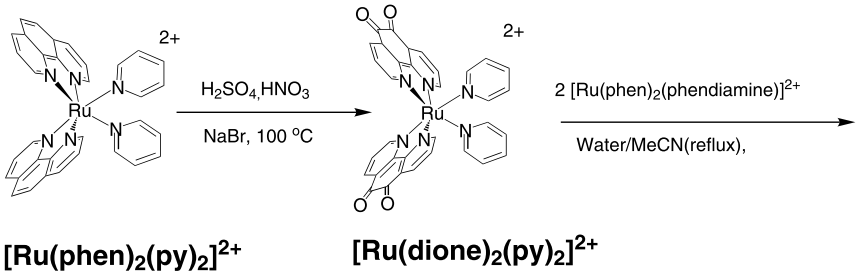

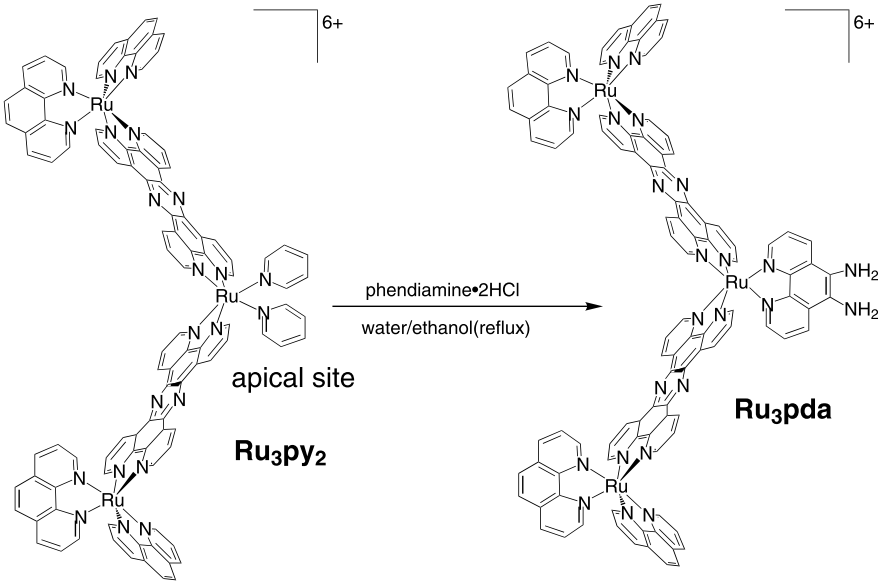

Fig. 11. Synthesis of trimeric building block, **Ru_3pda**.

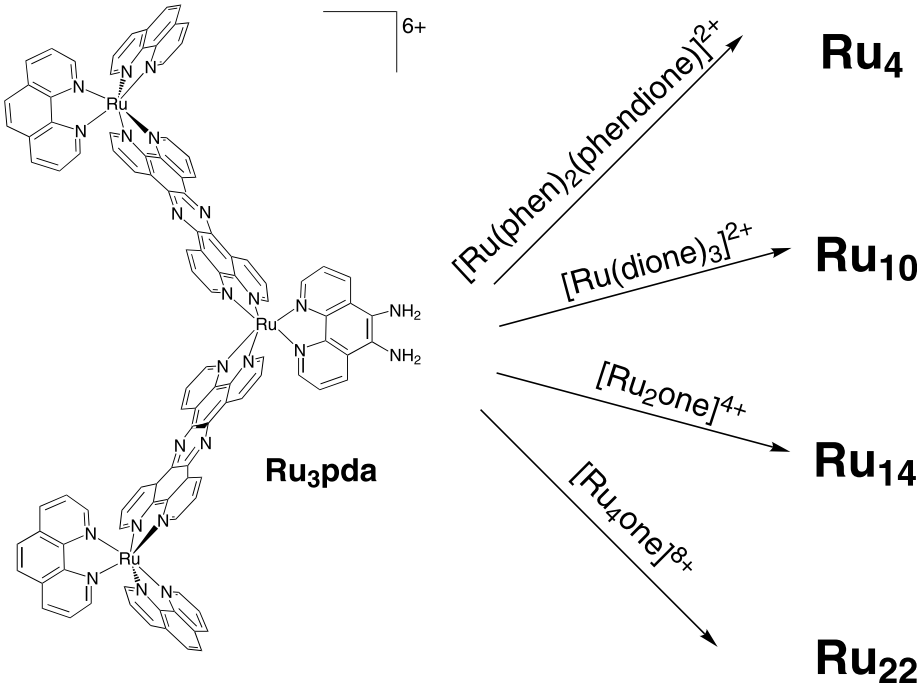

Fig. 12. Proposed convergent synthetic strategy for obtaining higher polynuclear dendritic metal complexes from **Ru_3pda**.

optical purity of this apical site as even a 10% 'impurity' will quickly add up in dendritic structure and dramatically effect the tertiary structures of the resulting dendrimers.

While **Ru_3pda** has been characterized by NMR, mass spectrometry and elemental analyses, there was a question as to whether the 1,10-phenanthroline-5,6-diamine ligand was bound via the phen 1,10-nitrogens or via formation of the 5,6-diimine [34]. Reaction of **Ru_3pda** and with $[Ru(phen)_2(phendione)]^{2+}$ yields only the expected tetramer **Ru_4** confirming the coordination via the 1,10-phen nitrogens. We are currently working at improving the optical purity at the apical Ru center on **Ru_3pda** and believe that once an optically pure trimer is prepared we will be able to access higher nuclearity dendrimers, such as a **Ru_{14}** and **Ru_{22}**, via the routes shown in Fig. 12, as well as prepare larger quantities and other stereoisomers of the already familiar **Ru_4** and **Ru_{10}**.

6. Summary

The development of a completely abiotic set of robust nanostructures which show hierarchical structure suggests that we may find new ways to organize 'nanomolecules' over much larger scales, from the mesoscopic to microscopic. Here, the primary structure is the stereochemical sequence. Secondary structure is exemplified by the presence of four-metal triangular planes. The global structure is analogous to the tertiary structure of a monomeric protein and the observed colloidal behavior (strong dependence of tertiary structure) suggests that specific aggregates arise in solution giving rise to quaternary structure. The synthetic chemistry is at this point well-established and we can truly begin to explore the effects of subtle changes in primary structure of the quaternary structures that arise. We continue to explore the ramifications and uses of these structurally precise, nanoscopic molecules and to develop new ways to construct even more complex architectures. Ultimately, we aim to use such structures as nanoscopic platforms from which to organize and construct mesoscopic 'arrays' of nanomolecules.

Acknowledgements

We thank Dr. Brad Herbert and Ms. Holly Carpenter of North Georgia College and State University and Professor John Wheeler of Furman University for their work on the CE of the dimers. We also Ms. Hongxia Zeng, Professor Zoltan Schelly and Ms. Thamara Janaratne of the University of Texas at Arlington for assistance with various experimental aspects of this work. This work was supported by the Robert A. Welch Foundation and the National Science Foundation (CHE-0101399).

References

[1] D.S. Goodsell, Am. Scientist 88 (2000) 230.

[2] D.S. Goodsell, A.J. Olson, Ann. Rev. Biophys. Biomol. Struct. 29 (2000) 105.
[3] D.S. Goodsell, A.J. Olson, Trends Biochem. Sci. 18 (1993) 65.
[4] J.-M. Lehn, Angew. Chem. Int. Ed. Engl. 27 (1988) 90.
[5] J.-M. Lehn, Supramolecular Chemistry, Concepts and Perspectives, VCH, New York, 1995.
[6] H. Sirringhaus, P.J. Brown, R.H. Friend, M.M. Nielsen, K. Bechgaard, B.M.W. Langeveld-Voss, A.J.H. Spiering, R.A.J. Janseen, E.W. Meijer, P. Herwig, D.M. De Leeuw, Nature 401 (1999) 685.
[7] V. Percec, M. Glodde, T.K. Bera, Y. Miura, I. Shiyanovskaya, K.D. Singer, V.S.K. Balagurusamy, P.A. Heiney, I. Schnell, A. Rapp, H.-W. Spiess, S.D. Hudson, H. Duan, Nature 419 (2002) 384.
[8] E.W. Meijer, A.P.H.J. Schenning, Nature 419 (2002) 353.
[9] M. Fujita, Chem. Soc. Rev. 27 (1998) 417.
[10] P.J. Stang, Chem. Eur. J. 4 (1998) 19.
[11] G.R. Newkome, C.N. Moorefield, F. Vögtle, Dendritic Molecules. Concepts, Syntheses, Perspectives, VCH, Cambridge, 1996.
[12] H. Mekelburger, W. Jaworek, F. Vögtle, Angew. Chem. Int. Ed. Engl. 31 (1992) 1571.
[13] P. Murer, D. Seebach, Angew. Chem. Int. Ed. Engl. 34 (1995) 2116.
[14] J.F.G.A. Jansen, E.W. Meijer, E.M.M. de Brabander-Van den Berg, J. Am. Chem. Soc. 117 (1995) 4417.
[15] H.-F. Chow, T.K.-K. Mong, M.F. Nongrum, C.-W. Wan, Tetrahedron 54 (1998) 8543.
[16] J.M. Frechét, Science 263 (1994) 1710.
[17] S. Campagna, G. Denti, S. Serroni, A. Juris, M. Venturi, V. Ricevuto, V. Balzani, Chem. Eur. J. 1 (1995) 211.
[18] K.L. Wooley, C.J. Hawker, J.M.J. Fréchet, J. Am. Chem. Soc. 113 (1991) 4252.
[19] D.A. Tomalia, A.M. Naylor, W.A. Goddard, Angew. Chem. Int. Ed. Engl. 29 (1990) 138.
[20] F.M. MacDonnell, M.-J. Kim, S. Bodige, Coord. Chem. Rev. 185–186 (1999) 535.
[21] F.M. MacDonnell, M.M. Ali, M.-J. Kim, Comm. Inorg. Chem. 22 (2000) 203.
[22] M.-J. Kim, F.M. MacDonnell, M.E. Gimon-Kinsel, T. DuBois, N. Asgharian, J.C. Griener, Angew. Chem. Int. Ed. 39 (2000) 615.
[23] F.M. MacDonnell, S. Bodige, Inorg. Chem. 35 (1996) 5758.
[24] J. Bolger, A. Gourdon, E. Ishow, J.-P. Launay, J. Chem. Soc. Chem. Commun. (1995) 1799.
[25] C.M. Shelton, K.E. Seaver, J.F. Wheeler, N.A.P. Kane-Maguire, Inorg. Chem. 36 (1997) 1532.
[26] K. Wouters, F.M. MacDonnell, Unpublished results.
[27] R. Konduri, M.-J. Kim, F.M. MacDonnell, manuscript in preparation.
[28] M.-J. Kim, R. Konduri, H. Ye, F.M. MacDonnell, F. Puntoriero, S. Serroni, S. Campagna, T. Holder, G. Kinsel, R. Rajeshwar, Inorg. Chem. 41 (2002) 2471.
[29] R. Konduri, H. Ye, F.M. MacDonnell, S. Serroni, S. Campagna, K. Rajeshwar, Angew. Chem. Int. Ed. 41 (2002) 3815.
[30] K. Wärnmark, O. Heyke, J.A. Thomas, J.-M. Lehn, Chem. Commun. (1996) 2603.
[31] R.D. Gillard, R.E.E. Hill, R. Maskill, J. Chem. Soc. (A) (1970) 1447.
[32] R.D. Gillard, R.E.E. Hill, R. Maskill, J. Chem. Soc. (A) (1970) 707.
[33] A.S. Torres, D.J. Maloney, D. Tate, F.M. MacDonnell, Inorg. Chim. Acta 293 (1999) 37.
[34] M.-J. Kim, Chiral metallodendrimers and oligomers containing Ru(II) polypyridyl complexes, in: Chemistry and Biochemistry, University of Texas at Arlington, Arlington, TX, 2000.
[35] D.J. Maloney, F.M. MacDonnell, Acta Crystallogr. Sect. C C53 (1997) 705.
[36] D.J. Maloney, F.M. MacDonnell, Acta Crystallogr. Sect. C C53 (1997) 705.
[37] S. Campagna, A. Giannetto, S. Serroni, G. Denti, S. Trusso, F. Mallamace, N. Micali, J. Am. Chem. Soc. 117 (1995) 1754.
[38] G.R. Newkome, C.N. Moorefield, Advances in dendridic macromolecules, in: G.N. Newkome (Ed.), Advances in Dendridic Macromolecules, vol. 1, JAI Press, Greenwich, CT, 1994.
[39] B. Bosnich, F.P. Dwyer, Aust. J. Chem. 19 (1966) 2229.
[40] S. Bodige, F.M. MacDonnell, Tetrahedron Lett. 38 (1997) 8159.
[41] X. Hua, A. von Zelewsky, Inorg. Chem. 34 (1995) 5791.
[42] X. Hua, A. von Zelewsky, Inorg. Chem. 30 (1991) 3796.
[43] T.J. Rutherford, M.G. Quagliotto, F.R. Keene, Inorg. Chem. 34 (1995) 3857.
[44] T.J. Rutherford, O. Van Gijte, A. Kirsch-De Mesmaeker, F.R. Keene, Inorg. Chem. 36 (1997) 4465.
[45] T.J. Rutherford, P.A. Pellegrini, J. Aldrich-Wright, P.C. Junk, F.R. Keene, Eur. J. Inorg. Chem. (1998) 1677.
[46] B.T. Patterson, F.R. Keene, Inorg. Chem. 37 (1998) 645.
[47] F.R. Keene, Coord. Chem. Rev. 166 (1997) 121.
[48] R.T. Watson, J.L. Jackson Jr., J.D. Harper, K.A. Kane-Maguire, L.A.P. Kane-Maguire, N.A.P. Kane-Maguire, Inorg. Chim. Acta 249 (1996) 5.